JET-P(94)65

JET Relevance to ITER, New Trends and Initial Results

The JET Team
presented by
J Jacquinot.

JET Joint Undertaking, Abingdon, Oxfordshire, OX14 3EA, UK.

Preprint of a paper to be submitted for publication in
Fusion Engineering and Design

December 1994

ABSTRACT

Critical ITER physics requirements and R & D issues are considered and, the relevance and capability of JET in investigating these issues are discussed. In particular, JET gives its highest priority to a coherent programme in support of the design of an ITER divertor operating in a regime consistent with a small scrape-off length. JET intends to perform critical tests of such divertor regimes in D/T plasmas. Initial results from JET after its extensive modifications are presented. These show that the new divertor in JET has good power handling capability and carbon blooms, that often plagued the earlier campaign of high performance, have not yet been observed. Good progress in divertor characterisation and, in achieving the H, VH-modes and full LHCD non-inductive current drive has been made. Also, a valuable insight into the ELM behaviour and their occurrence is being gained.

1. INTRODUCTION

Despite the very significant progress made in the nuclear fusion research in the last few years, the extrapolation from JET [1] and other large tokamaks to a fusion reactor still requires test of a series of concepts, materials and technologies for the successful realisation of an environmentally safe and potentially limitless source of nuclear fusion power. A major step in this direction is an international collaborative effort leading to the now Engineering Design Activity [2] of an International Thermonuclear Experimental Reactor (ITER-EDA). One of the aims of ITER is to demonstrate controlled ignition and extended burn (1000 s) of deuterium-tritium plasma. The outline conceptual design of ITER is fairly conservative with regard to reaching ignition. Nevertheless, to achieve this goal, it identifies a number of high priority physics and engineering issues requiring research and development (R & D) before the construction of ITER.

The main ITER physics R & D issues [2] are:

(i) Divertor: Particle and Power Exhaust
(ii) Confinement and Extrapolation to Ignition
(iii) Heating and Fuelling
(iv) Burn, Plasma Instabilities and Control.

The JET plasma is the closest to that of ITER. Its large size and high temperature allow access to regimes of low collisionality and small normalised gyro-radius which would prevail in ITER plasmas. The JET design and auxiliary equipment permit a wide range of operational modes including, most notably, the operation in a deuterium-tritium mixture. JET contributions to ITER issues are therefore important. In fact, JET already has a co-ordinated divertor physics programme [3] not only to satisfy the requirements of the JET high-performance D/T operation but also geared to provide important input in support of a successful ITER divertor design.

With a long term view of a fusion reactor, there is a significant scope of improvement [4] in the tokamak concept to achieve steady-state operation. These concept improvements require an optimisation of the plasma shape (triangularity and elongation) and the current density profile as a prerequisite to the attainment of high confinement regimes in stable plasmas. Coherent steady-state regimes of a tokamak reactor require an operation with large bootstrap current fraction combined with a seed current by an external source. The MHD stability of the discharge is achieved by using current profile control. Again, JET has the flexibility and capability of exploring such concepts in depth including the unique contributions that JET can make with its operation in such high performance D/T plasmas.

JET resumed plasma operation [5] in March 1994 after a shutdown of about two years. During this major shut-down, the machine, the data acquisition and the plasma position and control system have been extensively modified [6] including the installation of four divertor coils inside the machine to produce single-null pumped divertor plasmas. Auxiliary heating systems (ICRH, NBI, LHCD) have been modified/upgraded, in-vessel saddle coils for disruption control have been installed and a large number of new divertor and bulk plasma diagnostics have been introduced.

The paper is organised as follows. First, in section 2, we discuss the ITER physics issues mentioned above. In section 3, we present longer term issues on tokamak concept improvement and a coherent steady-state operation. In section 4, we outline the modifications of the JET device that can effectively be called "New JET" and we present a brief summary of the initial results obtained with the new JET. The conclusions of this paper are contained in section 5.

2. ITER PHYSICS ISSUES

2.1 Divertor: Power and Particle Exhaust

The main approach to power handling and particle exhaust in ITER will be to use a divertor. The divertor is also required to provide impurity control and a rapid recirculation of tritium in the device [7]. The plasma heat and particles crossing the separatrix, flow along the open field lines to the target plates. For a reactor producing fusion power of 3 - 4 GW, the heat load on the target could be as high as 100 MWm^{-2}. For ITER operation even with the reduced output of 1.5 GW, the power load on a "conventional" high recycling (attached) divertor is too excessive to survive. In a solution proposed for a high density divertor [7], the scrape-off layer plasma is extinguished (detached) before reaching the target plates in which energy and particle momentum are redistributed in the target chamber including the side walls by radiation and charge exchange processes.

JET has a coherent divertor programme in support of the design of an ITER divertor including the divertor modelling and model validation which at the same time fulfils the aim of JET of producing low impurity, long duration high performance D/T plasmas. Three types of divertors [3] (see Fig 1) are considered in the JET programme:

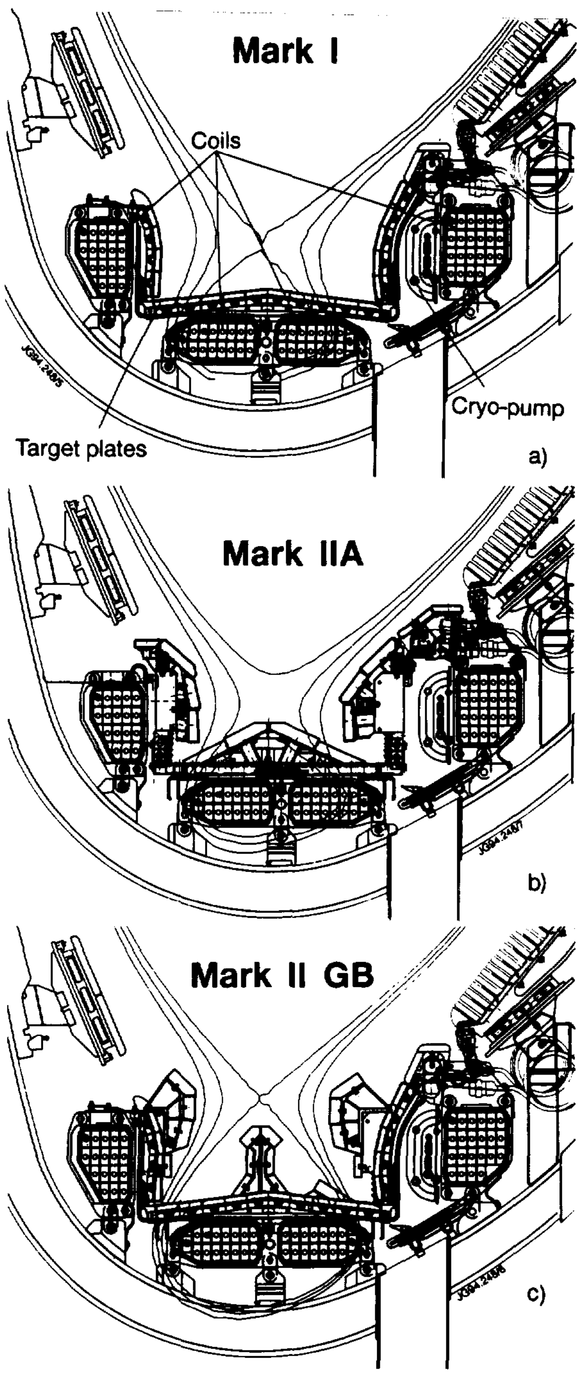

Fig 1 Three JET divertor configurations in support of ITER: (a) Mark I (installed in 1994 and operating). (b) Mark IIA (to be installed in 1995). (c) Mark II GB (to be installed in 1997).

(i) Mark I is a relatively open, inertially cooled divertor which incorporates X-point sweeping for high energy, high power load handling. This is presently installed in JET for the 1994-95 campaign and has already handled 140 MJ of plasma energy without carbon blooms.

(ii) Mark IIA (proposed for installation in 1995) is a moderate slot divertor (domed horizontal plates) that allows high power, high energy operation without the need of sweeping. In this more closed configuration, the pumping efficiency is improved and it should perform better with respect to impurity control and access to the radiative regime. The effect of orientation of the target on the escape of recycled neutrals will also be studied.

(iii) Mark II GB, presently at design level, would test a specific ITER "Gas Box" [7] concept using the same divertor support structure as the Mark IIA. Theconcept relies on the scrape off layer (SOL) plasma being extinguished (detached) before reaching the target plates. In this regime, a large cold region with $T_e < 3$ eV is formed throughout the divertor with reduced ionisation. Under these conditions, energy and momentum volume losses are particularly effective.

2.2 Confinement and Extrapolation to Ignition

The basic engineering parameters of ITER-EDA [2,8] are given in Table 1 although there may well be some small changes in their values as the EDA progresses. The performance of ITER with the above parameters has been evaluated using several models including the critical electron temperature gradient model [7] and empirical models of L-mode (ITER89-P) and H-mode (ITERH93-P) confinement. An 'H-mode amplification factor' (H) ~ 2 over the above

Parameter	Units	JET		ITER/EDA
		Original 1983-91	Divertor 1994 onwards	
Typical major radius	m	2.96	2.85	8.1
Typical minor radius	m	1.2	0.95	3
Plasma elongation		1.6	1.8	1.6
Toroidal magnetic field on axis	T	3.45	3.6	5.7
Plasma current	MA	≤ 7	≤ 6	24
Flat top pulse length	s	20 - 60	20 - 60	1000
Transformer flux	Wb	34	42	608
NBI power	MW	20	22	Heating methods to be chosen
ICRH power	MW	15	20	
LHCD power	MW	3(1991)	10	
ECRH power	MW	-	-	
Divertor Configuration		(SN(D), (SN(U), (DN)	(SN(D), (SN(U), (DN)	SN(D)

Table 1: JET and ITER Parameters

L-mode confinement would lead to ignition in ITER assuming $\tau_p/\tau_E = 15$, $n_{Be}/n_e \simeq 0.01$ and $< T_e > = 9$ keV producing a fusion power of about 1.5 GW. This power is calculated to be produced at $< n_e = 0.8 \times 10^{20}$ m^{-3} and at the Troyon factor g or the (normalised) β_N well below the limit of $\beta_N = 3$. Here, τ_p and τ_E are the particle and energy confinement times respectively.

In order to achieve H-mode confinement, a minimum (or threshold) power is required. The data base [9] of H-mode threshold assembled from tokamaks operating in deuterium is given in Figs 2(a) and (b). The deduced scaling can be represented as (a) $P_{th} \sim n_e^{0.75} B_T S$ or equally well by (b) $P_{th} \sim n_e B_T R^{2.5}$ where S represents the plasma surface area and the other symbols have their usual meaning. For an $< n_e > = 0.8 \times 10^{20}$ m^{-3}, a total heating power of 100 - 200 MW is required to achieve an H-mode in ITER. Note that the above scaling has not taken into account any improvement that may be obtained due to isotopic mass in the D/T operation. We remark that an improvement in energy confinement has been observed in circular TFTR plasmas in D/T mixtures [10] as compared to that in deuterium. In order to reduce the H-mode threshold power to a more acceptable level, clearly, some start-up scenarios have to be found with lower n_e and smaller S. Once the ignition is achieved, one needs to ensure helium ash removal. Fortunately edge localised modes (ELMs) develop spontaneously after a transition to the H-mode. ELMs expel plasma particles periodically and prevent impurity accumulation without an excessive loss of confinement. Much is to be understood of the physics of ELMs and their compatibility with divertors. ELM behaviour in large D/T divertor plasmas remains to be explored.

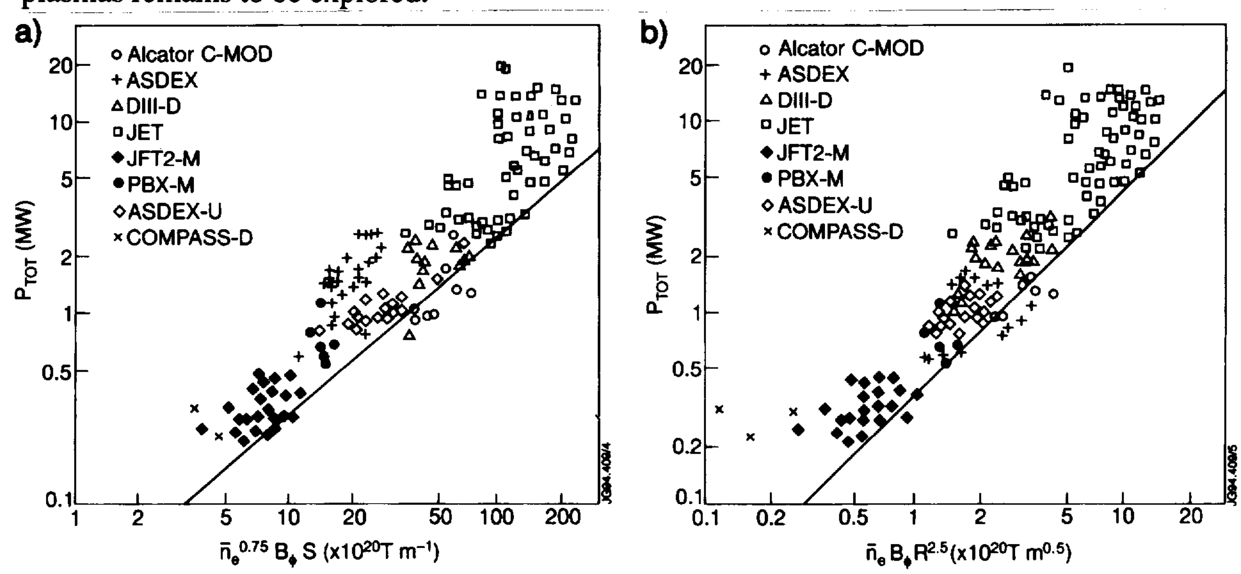

Fig 2 (a) H-mode power threshold vs $n_e^{0.75}$ $B_T S$ in a log-log plot using data from several tokamaks. (b) H-mode threshold vs $n_e B_T R^{2.5}$ in a log-log plot for the same data. Courtesy Ref. 9.

2.3 Heating and Fuelling

The primary aim of the auxiliary heating power in ITER is to achieve ignition. A secondary role of this system would be to exploit current drive and profile control in steady-state scenarios which utilise the high bootstrap current regimes requiring an externally provided central seed current. For additional heating in ITER, ICRH and NBI systems are the two leading candidates though ECRH is also being considered as well since it has an added advantage of assisting in plasma start-up. A significant additional heating database for the former two exist and JET has made a significant contribution to this database with combined heating powers up to 35 MW and plasma currents up to 7 MA [11]. The ICRF system has the capability of current profile and sawtooth control (via minority current drive) [12] whereas the beams can provide rotation of the plasma to prevent disruptions at low plasma density that may be caused by small error-fields. Edge fuelling (gas puffing and wall recycling) would be sufficient to fuel the core of ITER because particle transport is much faster than fusion burn-up. Shallow pellet injection can serve the purpose of density profile control in outer parts of the plasma but central fuelling by pellets require injection at high velocities which are as yet impossible to achieve. Core fuelling by neutral beam injection is not compatible with the tokamak energy balance [13] for ignited burn.

Plasma heating experiments in D/T plasma are essential to provide the database for prediction of heating to ignition and α-particle physics. After the preliminary tritium experiments (PTE) in JET in 1991, TFTR is at present carrying out such a programme in this direction and JET is provisionally scheduled to perform further D/T studies in 1996 (DTE1) and 1999 (DTE2). JET D/T experiments will be both unique and essential to provide a basis of the isotopic effects in divertor plasmas (confinement, H-mode threshold, ELM behaviour and divertor radiative regimes in D/T).

2.4 The Burn Phase

A 1000 s long burn phase [14] requires the control of:

(i) an operating point at a given fusion power while satisfying the relevant physics and engineering constraints,

(ii) the stability of fusion power production by detection and feed-back stabilisation of thermal instabilities in the burn process and

(iii) the capability of terminating the fusion power production quickly in response to component failures and to avoid damage to the tokamak and possibly safety problems.

Several methods of burn control (point (ii)) under feedback such as modulating the auxiliary heating power, D/T fuel mix, impurity concentration and modulation of gas fuelling [15] have been proposed as potential candidates. The latter method may control the core plasma density but also modifies the edge density which is limited by the divertor operation constraints and density limit considerations. Another means that can supplement the other techniques of burn control is the control of central temperature of the plasma by sawteeth control using current profile modification by the minority ion current drive at the $q = 1$ surface [16].

The burn phase also requires avoiding impurity or helium ash accumulation. The ignition domain diminishes when the ratio τ_p/τ_E increases. It has been found that the occurrence of edge localised modes (ELMs) ejects particles periodically from the plasma thus preventing impurity accumulation. However, ELMs also deteriorate the confinement (the H-factor) and disturbs the operation of divertor. There is a need for a knob to control the ELMs but no clear candidate(s) for such a task has yet emerged.

The burn phase also requires avoiding plasma disruption. Disruptions can occur due to a multitude of causes. There are radiative collapses near the density limit, low-q and β-limit disruptions. Disruption can also occur during termination of additional heating. Giant ELMs can lead to vertical instability of the plasma leading to a disruption. Monster sawtooth can trigger locked modes followed by a disruption. There are ways to avoid most of these disruptions but the last two are the most difficult to control externally and strongly point towards using a moderate plasma elongation.

There is also a possibility of α-particle driven instability such as the Toroidal Alfvén Eigen (TAE) modes during the burn phase. Only a sparse database on such instabilities is available and there is a need to study them experimentally. JET is scheduled to study such instabilities by active excitation of the relevant MHD modes via saddle coils installed inside the machine.

3. LONGER TERM ISSUES

3.1 Steady-state Operation

The ultimate aim of ITER is to approach steady-state operation which can only be done if the plasma current is driven non-inductively. However, to drive the total current in ITER by external systems requires prohibitively large input powers such that the recirculating power fraction of the reactor output is close to unity [15]. Steady-state operation in ITER can be envisaged at high poloidal β (β_p) and q and low current (~ 12 MA). Theory predicts that the plasma generates by itself a free source of non-inductive current called the bootstrap current. Such a current is proportional to β_p. When β_p reaches 2, most of the current is driven non-inductively. JET and JT-60U experiments have shown that it is possible to obtain discharges with more than 70 % bootstrap current in accordance with theory. More unexpected was the observation of good confinement with $H \geq 3$. The current density profile remains centrally peaked despite the broad bootstrap current. In steady-state in ITER fast waves [17], NBI or

ECRH can provide 0.5 - 3 MA in the centre as the seed current and the remaining 10 MA can be driven by the bootstrap current.

Such a mode of a steady-state operation of a burning plasma at a reduced plasma current of 12 MA in ITER requires a very challenging set of conditions:

(i) $H \geq 4$, a factor of 2 higher than in conventional ITER offsets the factor 2 lower in current,

(ii) a $\beta_p \sim 2 - 3$ to maximise the bootstrap current fraction,

(iii) $\beta_N > 3$ with a $q_{cyl} \sim 4$ and

(iv) the current drive efficiency factor $\gamma \geq 0.4 \times 10^{20}\, AW^{-1}\, m^{-2}$ to limit the power required for the seed current drive system.

Such a configuration of ITER is likely to operated [4] at $\beta_p \sim 3$, $q_{cyl} \sim 4$ and $I_p = 12$ MA whereas the conventional ITER is scheduled to operate at $\beta_p \sim 1$, $q_{cyl} \sim 2$ and $I_p = 24$ MA. Here, q_{cyl} is the equivalent cylindrical safety factor of a non-circularly shaped tokamak plasma.

The MHD stability for high β_N- values is obtained in the 2nd-stability domain which requires non-monotonic current profile that must be maintained in steady-state. The potentially limiting MHD instability is the low-n 'infernal' mode which is driven unstable by the pressure gradient in the low shear region around the minimum q rational surfaces [18]. In the steady-state, the external kink mode can become important when the bootstrap current drives a large edge current density. A large toroidal rotation may be necessary to ensure wall stabilisation of these modes. Ballooning modes are essentially stable in the negative shear region and the plasma core has access to the second stability regime. Outside the region of negative shear, the pressure gradient is limited by ballooning modes [18].

3.2 Capability and New Trends in JET

JET has the capability of investigating experimentally the scenarios discussed in the previous section with its significant battery of profile shaping tools which include fast-wave, lower hybrid and neutral beam auxiliary systems (see Table 2). In addition to the already achieved results in JET (VH-modes, large bootstrap current, PEP + H-modes), a programme of study of such steady-state tokamak regimes is considered in JET. Such a programme includes the establishment of long plasma pulses with high bootstrap fraction, control of current and pressure profiles and seed current drive. A full-scale transport code simulation with non-inductive current drive profiles obtained from lower hybrid, fast wave and neutral beams in conjunction with the naturally occurring bootstrap current are used [19] to predict the discharge evolution, its stability and performance. These calculations indicate that plasmas with steady-state non-monotonic current profiles can be produced in JET.

System	Power	Pulse Length	Current Drive $n_e = 4.10^{19}$ m^{-3} $T_e = 7$ keV
NBI (deuterium)	13.6 MW/85 keV 7.6 MW/140 keV	10 s	0.015 AW
ICRH/FWCD	20 MW/23-55 MHz	20 s	0.04 A/W
LHCD	10 MW/3.7 GHz	20 s	0.2 A/W

Table 2: Heating and Current Drive Systems Installed on JET

4. INITIAL RESULTS OF NEW JET

4.1 The New JET

A view of the interior of the vacuum vessel of the new JET after its extensive modifications [6] is shown in Fig 3(a). The major modifications include the water-cooled divertor target plates (in CFC) located at the bottom of the machine. Four divertor coils (see Fig 3(b)) powered individually and located inside the vacuum vessel permit in conjunction with other poloidal field system a single null divertor plasma in which the X-point can be swept up to 4 Hz to spread the heat load on the target plates. A cryo pump (cooled by liquid nitrogen and liquid helium) is also provided (2000 l s^{-1}) in the divertor chamber for exhaust of neutrals that arrive at the mouth of the pump and it traps the D, T and most of the impurities effectively. Operation with Argon frost is foreseen to pump hydrogen and helium as well. The divertor configuration necessitated the new Ion Cyclotron Resonance Heating (ICRH) antennas [20] for which 4 new units of 4-strap each have been installed, with better directivity for Fast Wave Current Drive applications. The screen rods are made of beryllium and are aligned to the total B-field. These antennas have remote (~ 2.5 m) ceramic support [21] (for the coaxial feed line) simulating an ITER antenna feature. A number of poloidal limiters in CFC protect each antenna unit from the side. The upgrade of the LHCD system which includes a cryo pump is now capable of delivering 10 MW of power to the plasma. The NBI system has been upgraded to deliver deuterium beams to a level of up to 22 MW. A new NBI duct protection system has been installed which allows long pulses and operation at low plasma current up to 1 MA. A set of 4 saddle coils have been installed for disruption control studies and that of active TAE-mode

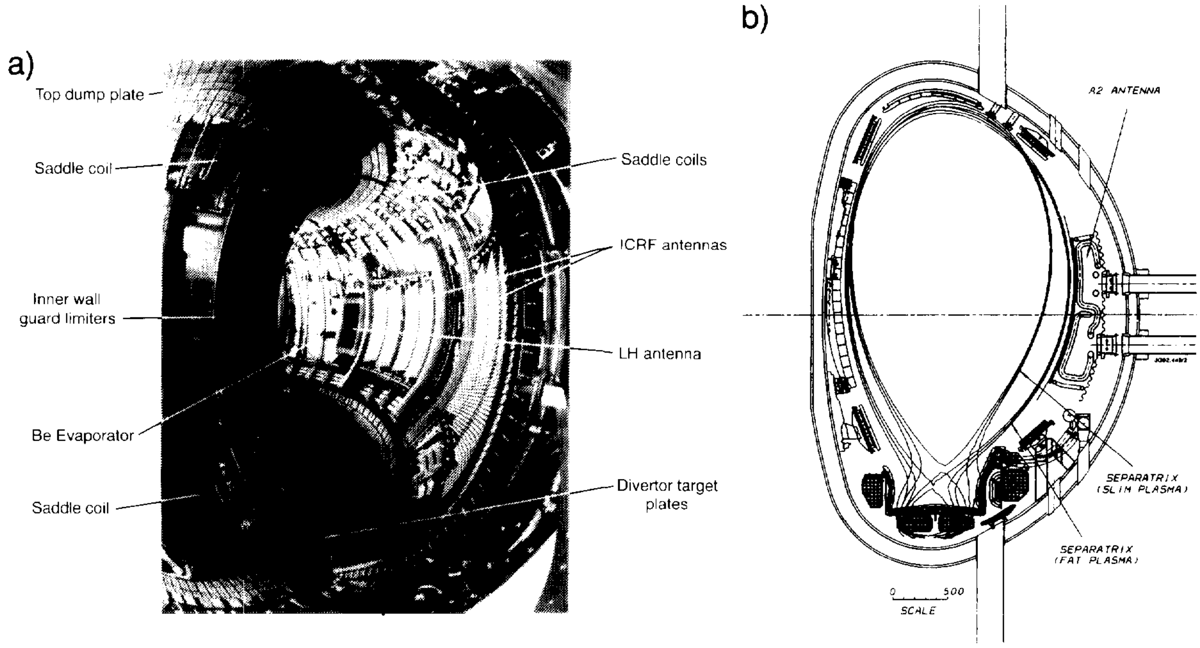

Fig 3 (a) A photograph of the interior of the modified JET in 1994 before closing the machine for pumpdown showing several important in-vessel components. (b) A poloidal cross section of the modified JET showing the divertor coils, target plates, cryo pump, ICRH antenna, poloidal limiter inside the vacuum vessel.

excitation. Glow discharge conditioning is used and beryllium evaporation is carried out for gettering purposes. For the divertor tile conditioning, high power helium tokamak discharges are also used. The tokamak operation is carried out with walls at 250°C.

A new Plasma Position Control Circuit (PPCC) [21] has been commissioned that uses a real-time plasma boundary measurement at 5 locations (poloidally) including the X-point position every 3 ms to control the shape of the plasma. Also, a fast (200 µs) radial field amplifier (FRFA) in conjunction with a digital controller system (sampling the vertical position every 50 µs) is used for the stabilisation of vertical position of the plasma.

4.2 Initial results

4.2.1 X-point sweeping and detached divertor plasmas

Single null X-point divertor discharges with a plasma current up to 4 MA at full field of 3.4 T have already been produced in this initial operation of new JET. With the help of the 4 divertor coils, a range of X-point configurations in which the height of the X-point can be varied from 0 to 40 cm and the power and particle load can be directed from horizontal (normal operation) to the vertical target plates of the divertor, have been produced [3]. As mentioned before, the X-point can be swept readily at a frequency of up to 4 Hz which permits the sweep of the strike point on the target plate of about 30 cm. The effect of sweeping on the tile temperature is shown in Fig 4. In the unswept duration, the tile temperature (infrared thermography) rises with the characteristic square-root time dependence. But, sweeping of the strike point allows to spread the heat load and, as shown in Fig 4, the rise in tile temperature is reversed when the sweeping commences. The sweeping, however, did not alter the ELM behaviour or their frequency. In high power ELMy H-modes, the use of sweeping has allowed a heat load on the target plates of 90 MJ with a surface temperature of 850°C whereas without sweeping the tile temperature rose to 1100°C with a heat load of 40 MJ. In the "old" (1991) JET configuration, carbon blooms occurred with an input energy of 10 -15 MJ in ELM-free H-modes and 70 MJ in ELMy H-modes.

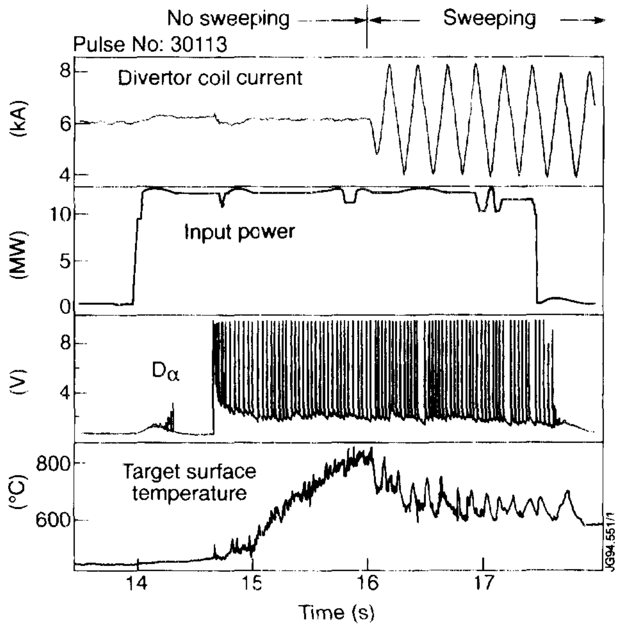

Fig 4 Time traces showing the effect of divertor X-point sweeping on the tile temperature in high power ELM-free and ELMy discharge.

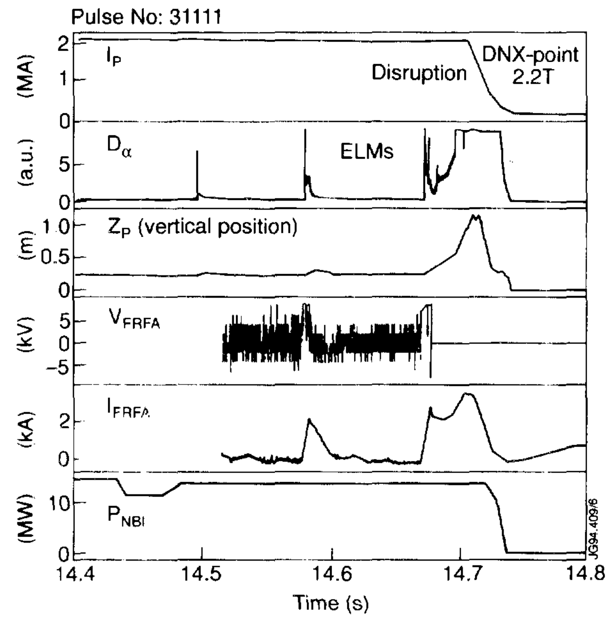

Fig 5 An illustration of vertical disruption induced by the occurrence of giant ELMs. Voltage and current of the fast radial field amplifier (FRFA) which are in the vertical position stabilisation feedback loop are as shown.

The coupling resistance of the ICRH antenna is only negligibly affected by sweeping as the plasma displacement near the mid-plane, where the antennas are located, is only mildly changed by sweeping. The occurrence of ELMs, however, changes the coupling on a rapid time scale (at the ELM frequency) which can affect the operation (tripping) of the ICRH generator system particularly when the coupling resistance is low. Note that ELMs are not harmful to the antenna itself as upon their occurrence, ELMs reduce the voltage on the antenna.

In some instances, giant ELMs can trigger vertical instability of the plasma for which we present an example in Fig 5. The giant ELMs at 14.49 and 14.59 s, induce a vertical motion of the plasma but the vertical position feedback control system which includes the fast radial feed amplifier (FRFA) copes with such perturbations. However, the vertical movement triggered by the giant ELM at 14.68 s could not be controlled and the plasma disrupted at 14.7 s, as seen from the figure. It is clear that a means of controlling ELMs/giant ELMs in highly elongated ($\kappa \simeq 1.9$) plasmas is of importance.

In Fig 6(a), we show the production of an ITER-relevant detached divertor plasma in an ohmic-heated discharge. The profiles of ion saturation current (Langmuir probes in the divertor region) around the separatrix near the inner and outer strike zones are also shown in Figs 6(b) and (c) for "detached" and "attached" time slices of the discharge. The ion saturation current falls at both strike zones before radiation increases at 11.55 s into the discharge. For detached plasmas, the peak ion saturation current occurs further away from the separatrix. Detachment is also confirmed by CDD camera, D_α and CII line intensity measurements.

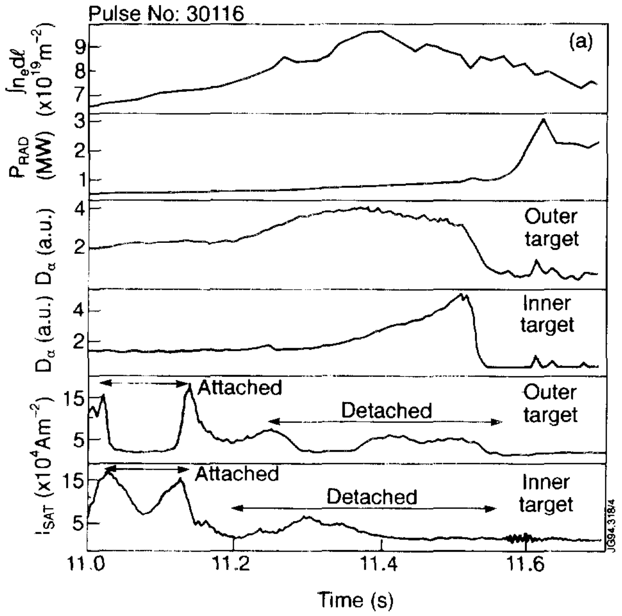

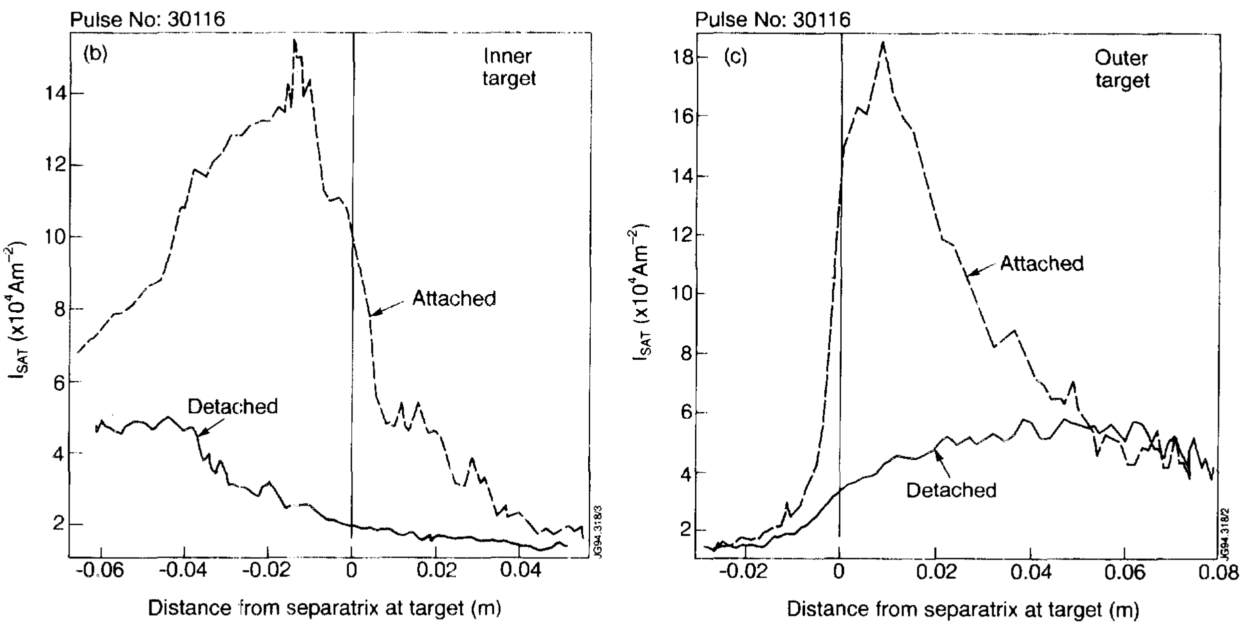

Fig 6 (a) Time traces of an example of attached and detached plasmas in JET Mark I divertor. (b) Profiles of Langmuir probes measured ion saturation current across the separatrix in the case of attached and detached plasmas at the inner strike zone. (c) Same as in (b) but for the outer strike zone

4.2.2 Pressure scrape-off lengths:

In Fig 7 (a), we show time traces of a high power (12 MW) ELMy H-mode discharge. For the same discharge we show a 3-D plots of tile temperature profiles in Fig 7(b) using the new infrared thermography diagnostic in JET that has a spatial resolution of 3.5 mm radially (averaging over 30 cm toroidally) and temporal resolution of 10 ms. We note that in this discharge, there is a large asymmetry in the power dumped at the inner and outer strike zones. But, depending on details in the flux expansion, there are cases where the

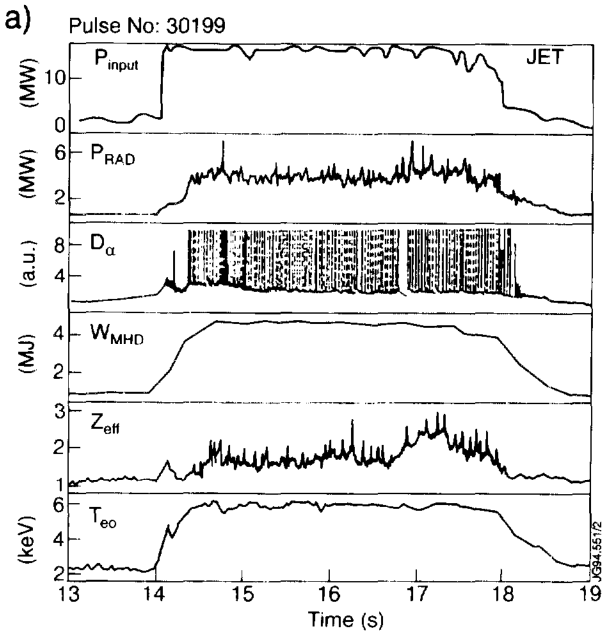

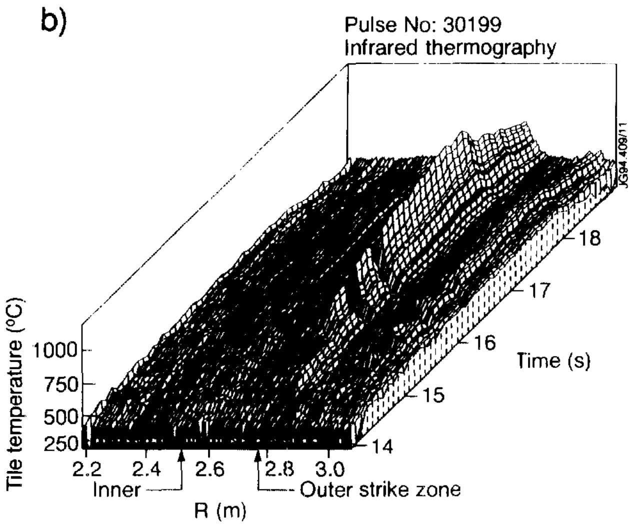

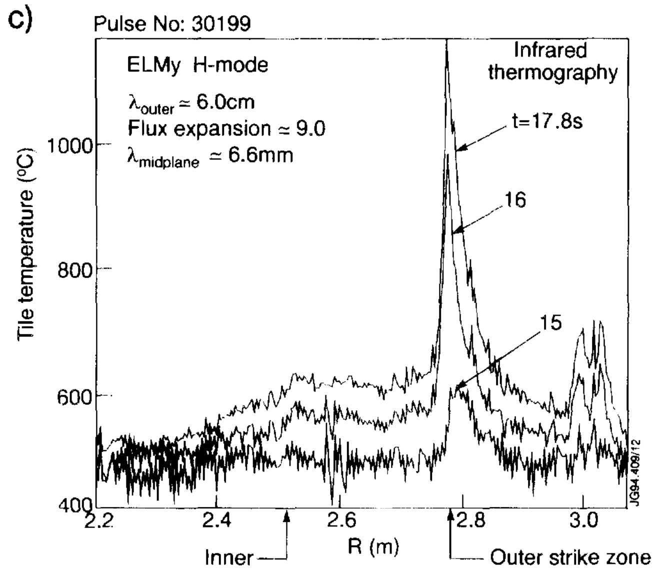

Fig 7 (a) Time traces of an ELMy H-mode discharge which is used to illustrate the power handling capability of the Mark I divertor by infrared thermography measurements shown in (b) and (c). (b) A 3-D plot of the divertor target tile temperature measured by high resolution infrared thermography for the discharge shown in (a). (c) A profile of tile temperature for three time slices showing an asymmetry at the inner and outer strike zones. Thermal or pressure scrape-off lengths can be deduced.

power is balanced or even the asymmetry is reversed [23]. Temperature profiles across the inner and outer strike zones for 3-time slices are shown in Fig 7(c) from which the thermal scrape off length can be deduced. The rise in tile temperature (from the base-line temperature measured by thermocouples) can be related to the power delivered to the target [23] and there is about 20 - 30% deficiency in power accounting when the radiated power is taken into account.

From these measurements, a pressure (density x temperature) scrape length can be deduced. This is estimated to be 6 cm in the divertor region which translates to 0.66 cm at the mid-plane taking the flux compression into account. This value is somewhat smaller than expected and emphasises the need for a radiative divertor in ITER.

4.2.3 H-mode behaviour

H-modes in discharges of plasma current up to 4 MA in JET have been achieved. In the initial operation, the H-modes have been dominated by ELMs and it has been observed that the ELM frequency increases as the input power is increased (see Fig 8). But, as conditioning of tiles progresses, longer ELM-free periods are obtained. Also, it appears that the ELM-free period increases with plasma current and is sensitive to recycling conditions and plasma shape.

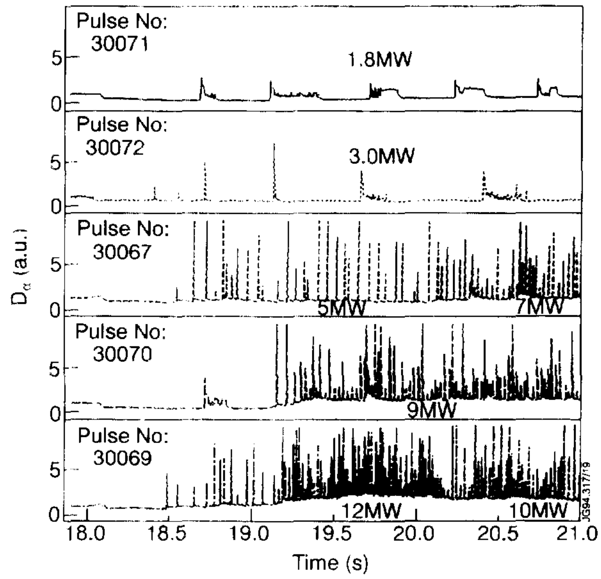

Fig 8 Time traces of D_α signal in several shots showing the occurrence of ELMs (frequency) as a function of power in divertor discharges. Frequency of ELMs increases with power.

In Fig 9(a), we present the confinement time behaviour of an H-mode obtained in a 2.5 MA, 2.8 T discharge at a power level of 14.5 MW. This discharge has an ELM-free period of about 0.95 s and then a series of ELMs are produced. The observed confinement time (diamagnetic) is compared as a function of time with ITERH93-P (H-mode scaling) [24] and ITER89-P (L-mode scaling) [25]. It is seen that the energy confinement agrees with L-mode scaling in the L-phase of the discharge. During the ELMs, the confinement corresponds to the H-mode scaling whereas in the ELM-free period, the confinement is about 20% higher than the H-mode scaling. In Fig 9(b), we compare the observed confinement in a series of ELMy H-mode discharges obtained in a range of I_p (2 - 3 MA) and B_T (2.3 - 3.4 T). On average, it is about 0.8 of the ITERH93-P (ELM-free) confinement scaling.

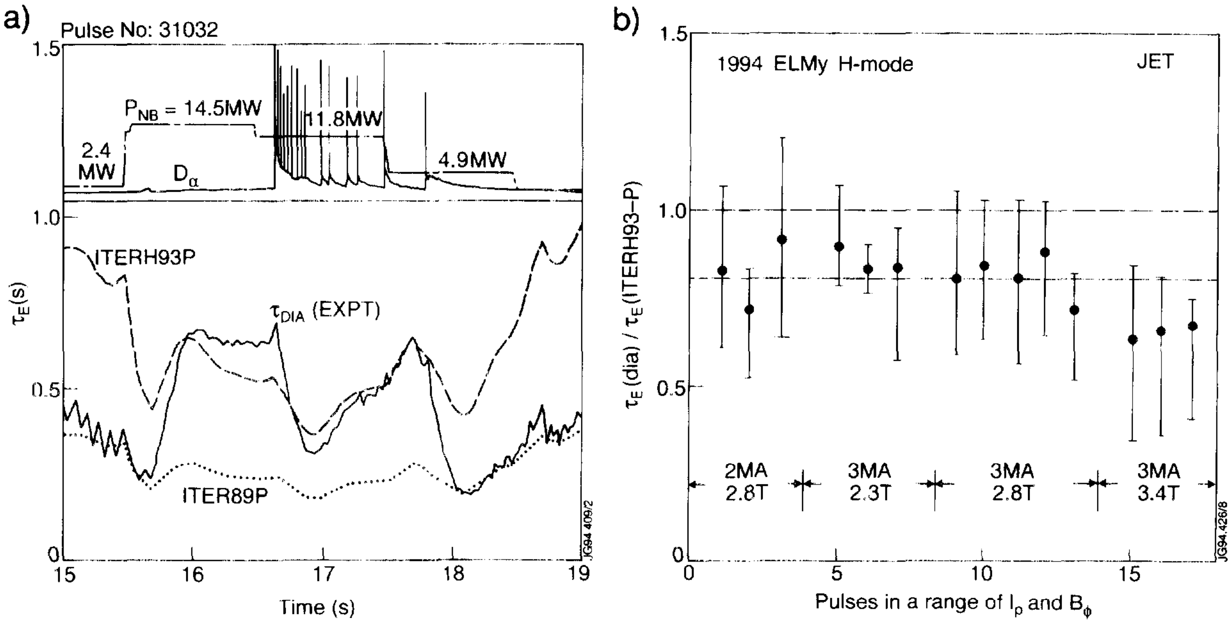

Fig 9: (a) Time traces of an H-mode discharge showing ELMs and ELM-free periods. Observed energy confinement time is compared with ITERH93-P (H-mode) and ITER89-P (L-mode) scalings. (b) observed energy confinement relative to ITER H93-P scaling in ELMy H-mode discharges in a range of plasma currents (2 - 3 MA) and toroidal fields (2.3 - 3.4 T).

In Fig 10(a), we present an hot-ion H mode discharge in which initially there was an ELMy period and then an ELM-free period of 0.55 s was obtained. The central ion temperature T_{i0} (charge-exchange recombination spectroscopy) rose to 18 keV and the maximum electron temperature T_{eo} was 8.5 keV whereas the volume averaged density $< n_e >$ was about 2.8 x 10^{19} m^{-3}, the maximum DD-reaction rate R_{DD} was 3.4 x 10^{16} s^{-1} and the diamagnetic energy confinement was about 35% higher than the ITERH93-P scaling leading into the VH confinement regime. As compared to similar discharges of 1991 (prior to preliminary tritium experiments (PTE)), the Z_{eff} is lower but the rate of rise of density during an ELM-free period is higher possibly due to the reduced plasma volume in this campaign and the shorter ELM-free period. The latter two may be limiting the neutron yield which was about a factor of 3 lower than in one of the best 1991 discharges.

A JET VH-mode database (old and new JET) of combined NBI and ICRF heating is shown in Fig 10(b) in the (T_{io} - T_{eo}) plane. Notice a discharge (data point encircled in

Fig 10(b) which shows a $T_{eo} \simeq 12$ keV with a $T_{io} \simeq 8$ keV [26]. This has been termed as a hot-electron VH-mode discharge obtained by a predominant ICRF heating. It is worth stressing that the same global confinement is obtained as that with NBI discharges having ten times more toroidal rotation. Time traces of such a discharge are shown in Fig 10(c) where an ELM-free period of 2.7 s was obtained with a VH confinement time of about 1 s.

In the new JET, the high β_p values obtained are no longer transient but reach "quasi

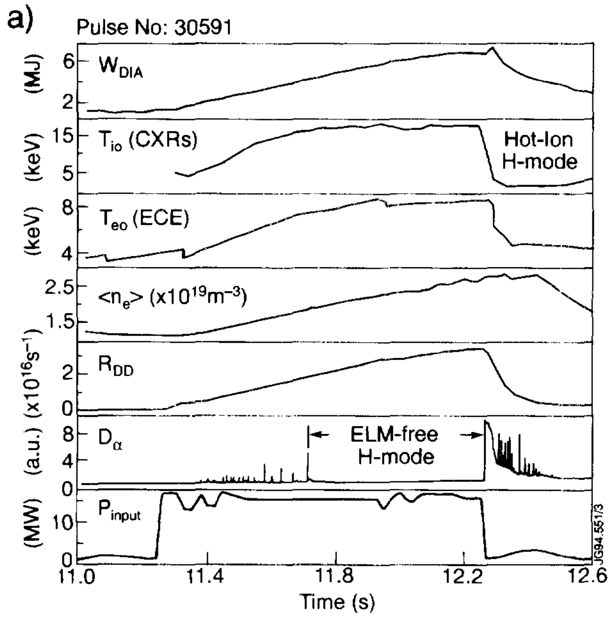

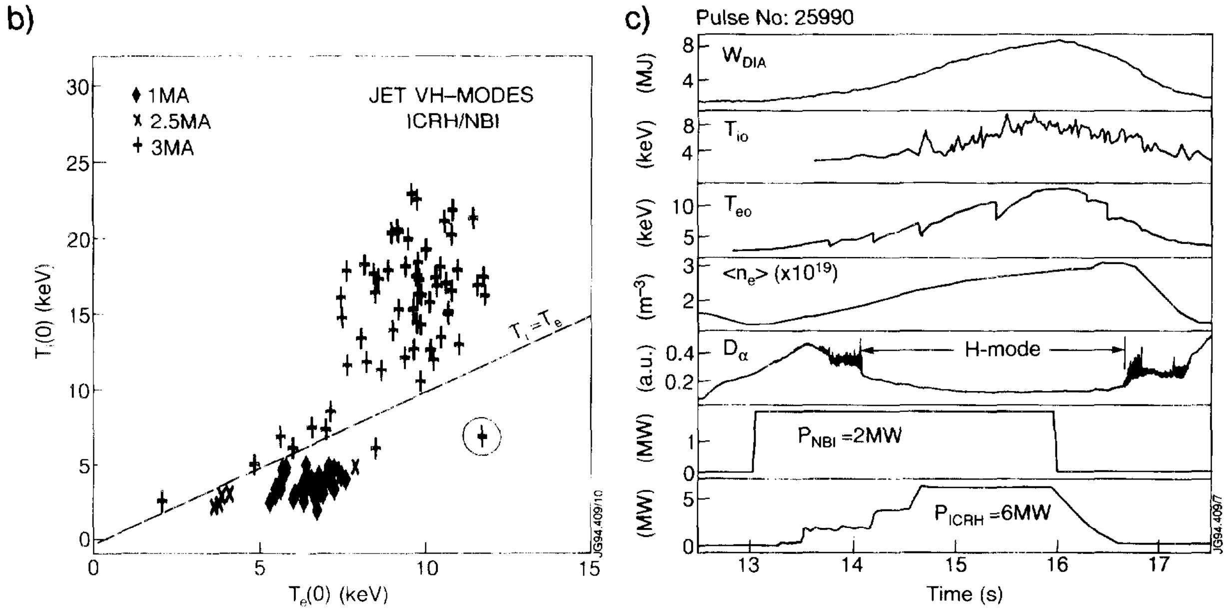

Fig 10: (a) Time traces of a hot-ion H-mode discharge showing ELMs and ELM-free periods. The ion temperature reached 18 keV and H ~ 2.3. (b) A data base of JET hot-ion and hot-electron H-mode obtained with NBI/ICRF heating. The data point encircled is the hot-electron VH-mode. (c) Time traces of the hot-electron VH-mode pointed out in (b). In this discharge, the ICRH was the dominant heating and $\tau_E \cong 1$ s.

steady-state" levels [27]. Time traces of a high β_p ELMy H-mode discharge ($\beta_p > 2.4$ for 2 s with a transient peak value of 2.8) is shown in Fig 11(a) with a total input power of 21.5 MW applied to a single null divertor plasma of 1 MA at $B_\phi = 2.8$ T. The energy confinement time is ~ 1.4 times the ITER H-mode scaling [24]. Although, the energy confinement time obtained until now falls short of the levels reached in VH-modes in 1991, the parameter domain for obtaining high performance has been considerably enlarged. High β_p data ($\beta_p > 1$) obtained in the new JET is plotted in a β_p vs q_{95} (safety factor at 95 % of the plasma radius) diagram and compared with 1991 data in Fig 11(b). Also drawn are the lines of normalised β (β_N = 2, 3 and 4) together with the region in which the low current steady-state reactor operation is envisaged. It is clear that we are approaching the regime required for such advanced reactor scenarios.

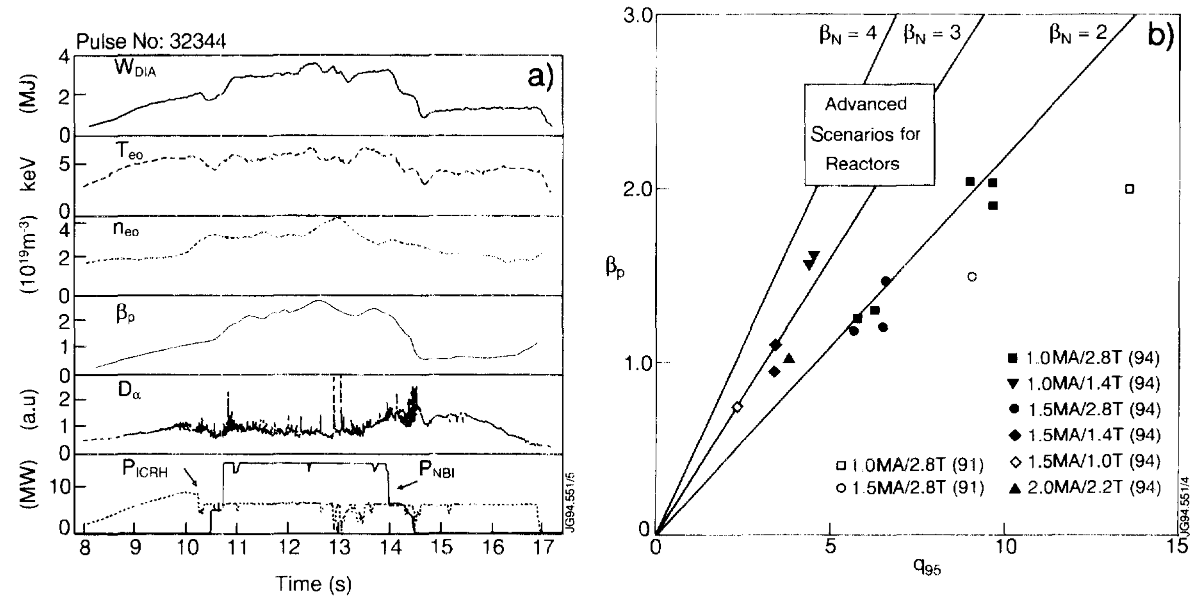

Fig 11: (a) Time traces of high β_p ELMy H-mode 1 MA discharge at B_ϕ = 2.8 T. W_{DIA} represents stored energy measured by a diamagnetic loop and other symbols have their usual meaning. (b) High β_p values obtained in JET discharges are plotted as a function of q_{95} (safety factor of 95% of the plasma radius). Also drawn are the lines of normalised β and the operating region of advanced reactor scenarios.

4.2.4 RF current drive

JET has achieved 2 MA non-inductive current drive by RF waves either by LHCD system alone or in combination with fast wave ICRF heating system. The LHCD system operates at 3.7 GHz and has a grill type launcher (48 multi-junctions) with 384 waveguides producing an $n_\parallel$-spectrum, the peak of which can be varied from 1.4 - 2.3 whereas the width of the spectrum (between adjacent minima) is 0.46. In Fig 12(a), we show time traces of a discharge in which full plasma current (2 MA) was sustained by LHCD [28] at a power level of 4 MW and at a central density of 2.3 x 10^{19}m^{-3} leading to a current drive efficiency factor $\gamma = 0.25 \times 10^{20}$ AW^{-1} m^{-2}. The non-inductive current drive effect is evidenced by the OH flux which remained fully flat as a function of time for about 4 s indicating that there was no ohmic flux consumption and that the current was being driven non-inductively. The decrease in plasma internal inductance l_i indicates that the current profile was flattening which is acharacteristic of LHCD as it drives less current on-axis. Similar current drive was also obtained with a combination of LHCD (4 MW) and ICRH (2.5 MW) at a similar density as before (see Fig 12(b)). The ICRH antennas were used in the non-synergy heating mode ((0,

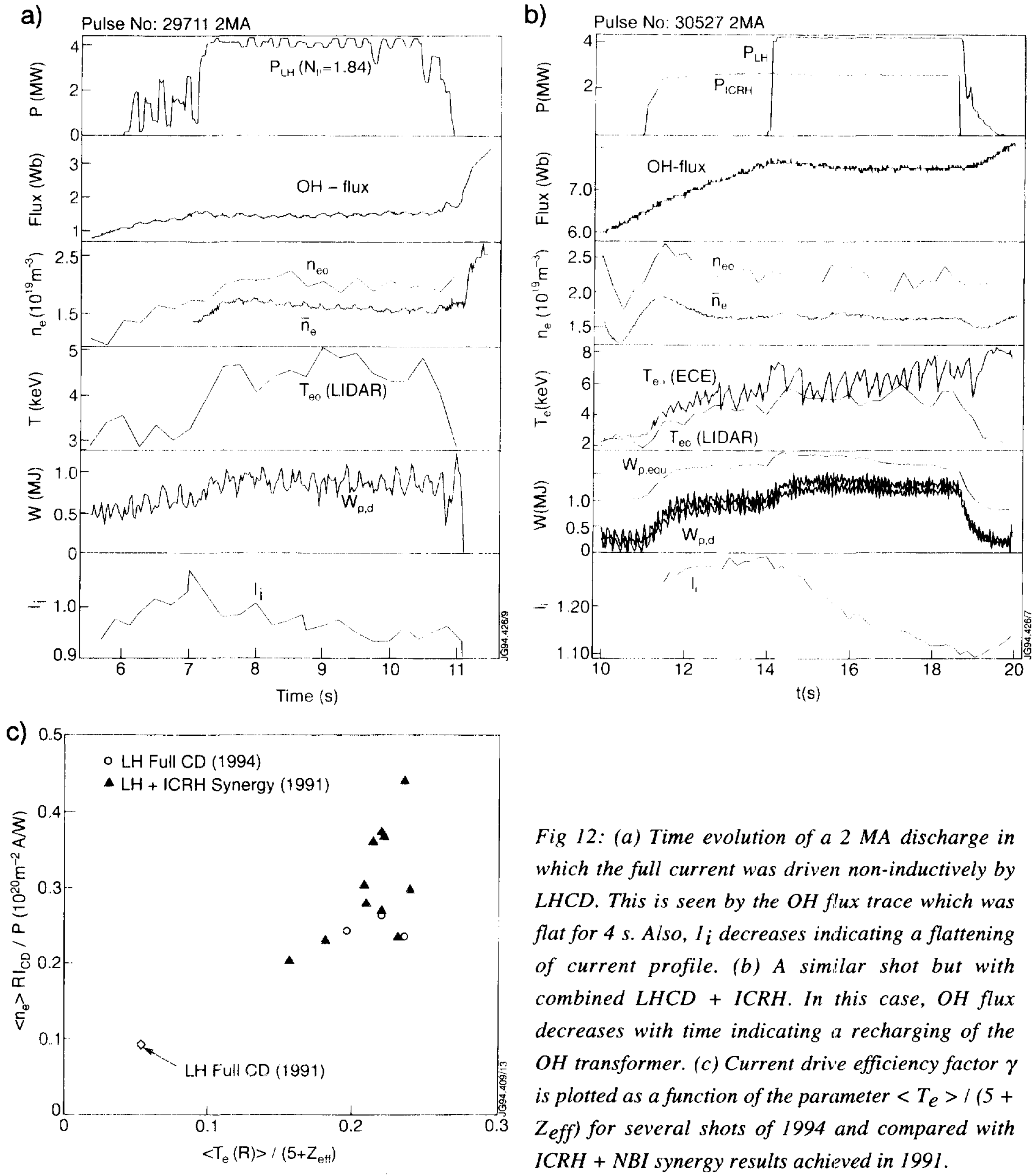

Fig 12: (a) Time evolution of a 2 MA discharge in which the full current was driven non-inductively by LHCD. This is seen by the OH flux trace which was flat for 4 s. Also, l_i decreases indicating a flattening of current profile. (b) A similar shot but with combined LHCD + ICRH. In this case, OH flux decreases with time indicating a recharging of the OH transformer. (c) Current drive efficiency factor γ is plotted as a function of the parameter $< T_e > / (5 + Z_{eff})$ for several shots of 1994 and compared with ICRH + NBI synergy results achieved in 1991.

π)-phasing). However, the increased electron temperature led to improved LHCD efficiency. In this case, the OH-flux instead of remaining flat decreased slightly with time indicating a recharging of the OH transformer.

In Fig 12(c), we present the current drive efficiency factor γ as a function of a characteristic parameter $< T_e >/(5 + Z_{eff})$ for the present full LHCD current drive cases which are compared with earlier (1991) synergy results of LHCD + ICRH in which the latter was used in (0, 0)-monopole phasing. The present LHCD values are in the same range except that in some cases the synergy can attain rather high values as γ as seen in Fig 12(c).

5. CONCLUSIONS

From earlier and most recent experiments, it is emerging that the scrape-off length in a tokamak is small ($\leq$ 1 cm in JET) and is not likely to increase with the size of the machine. It is, therefore, most likely that the divertor in ITER will have to work in the radiating (detached) regime in order to reduce the heat load on the target plates to an acceptable level. The physics and technology of such a divertor has to be demonstrated in the present day machines in order to support the divertor design on ITER. JET has a coherent programme to fulfil this task. Based on present day deuterium experiments, the power threshold for attaining an H-mode on ITER is high. TFTR results hint at more favourable values in D/T mixtures. This result places a strong emphasis on the study of H-mode threshold in D/T plasmas and on ignition routes passing via low threshold conditions. It appears that occurrence of ELMs forms an essential part of the tokamak operations and which affect the confinement and the operation of the divertor. A knob has to be found to control ELMs so that their favourable features such as ejection of particles could be utilised to its full extent in ash removal without affecting the divertor operation.

On a longer term basis, development of tokamak concepts such as high β_p, high bootstrap current and high confinement regimes should be pursued vigorously so that a reactor can be operated at a lower current which will also allow the steady-state operation. JET is well placed to carry out such a study in time to be incorporated in the later developments of ITER.

First results from the initial operation of JET show that the new divertor has a good power handling capability. The observed behaviour of ELMs (increasing frequency) with input power and longer ELM-free periods with increasing plasma current, recycling and plasma shape are giving a new physics insight possibly leading to their control. Confinement of ELMy H-modes is about 0.8 of the ELM-free (ITERH93-P) H-mode scaling. The hot-ion H-modes have been reproduced with VH-mode confinement characteristics. Full current drive has been achieved in a 2 MA plasma at $n_{eo} = 2.3 \times 10^{19}$ m^{-3} with LHCD and also in combination with ICRH.

ACKNOWLEDGEMENT

It is a pleasure to acknowledge the important contribution of Dr V Bhatnagar in the preparation of this paper.

REFERENCES

[1] Keilhacker, M.J. and the JET Team, in Plasma Phys. and Contr. Nucl. Fus. Res. 1992 (Proc. 14th Int. Conf., Wurzburg, Germany, 1992), vol. 1, IAEA, Vienna (1992) 15.

[2] ITER Director, ITER Outline Design, ITER Tech. Advisory Comm. (TAC-4), January 1994, ITER-JCT, Garching Germany.

[3] Watkins, M.L. and the JET Team, Proceedings 21st EPS Conf. on Contr. Fus. and Plasma Phys., Montpellier, France (1994), to appear.

[4] Thomas, P.R. and the JET Team, ibid.

[5] Tanga, A. and the JET Team, ibid.

[6] Bertolini, E. and the JET Team, these proceedings.

[7] Rebut, P.-H. et al., Fus. Eng. and Design, 22 (1993) 7.

[8] Parker, R.R. and the ITER Joint Central Team, Plasma Phys. Contr. Physics, 35, No. 12B (1993) B23.

[9] Ryter, F. and H-Mode Database Working Group, as in Ref. 3.

[10] Strachan, J., as in Ref. 3.

[11] Lomas, P. and the JET Team, as in Ref. 1, p. 181.

[12] Start, D.F.H. et al., Proceedings 19th EPS Conf. Innsbruck, 16C (1992) part II, 897.

[13] Bickerton, R.J., Dynamics of a Steady-state D/T Burning Tokamak Plasma, Report JET-R(92)03, JET Joint Undertaking, Abingdon (1992).

[14] Post, D.E. et al., ITER Physics, ITER Documentation Series 21, IAEA, Vienna, 1991.

[15] Rebut, P.-H., et al., Plasma Phys. Contr. Fus., 35 (1993) A3.

[16] Bhatnagar, V.P. et al., JET preprint JET-P(94)22, to be published in Nucl. Fus. (1994)

[17] Bhatnagar, V.P., Jacquinot, J. (Eds), Fast Wave Heating and Current Drive in ITER, NET Report 103, EUR-FU/XII/163/94 (1994), The NET Team, Garching, Germany.

[18] Holties, H.A. et al., as in Ref. 3.

[19] Soldner, F. et al., as in Ref. 3.

[20] Kaye, A.S., et al., Fus. Eng. and Design, 24 (1994) 1.

[21] Jacquinot, J. et al., Proceedings IAEA Tech. Comm. Meeting on RF Launchers in Large Devices, Naka, Japan (1993), to be published.

[22] Garribba, M. et al., these proceedings.

[23] Clements, S. et al., (1994) Private Communication.

[24] ITER H-Mode Database Working Group, Nucl. Fus., 34 (1994) 131.

[25] Yushmanov, P.N. et al., Nucl. Fus., 30 (1990) 1999.

[26] Jones, T.T.C., as in Ref. 3.

[27] Gormezano, C. and The JET Team, 15th IAEA Int. Conf. on Plasma Phys. and Contr. Fus., Seville, Spain, October, 1994.

[28] Soldner, F. and The JET Team, 15th IAEA Int. Conf. on Plasma Phys. and Contr. Fus., Seville, Spain, October, 1994.